



AVHRR analysis of a savanna site through a fire season in Brazil

H. FRANÇA and A. W. SETZER

National Space Research Institute of Brazil, INPE/DSR, C. Postal 515,
12201 S.J. Campos, SP, Brazil

(Received 8 March 1999)

Abstract. A temporal sequence of images from the Advanced Very High Resolution Radiometer (AVHRR) orbital sensor along 1.5 year was used to study the response of a savanna site that burnt in the dry season. The Emas National Park of Brazil was monitored with 1.1 km high resolution afternoon images from June 1992 to October 1993 through the responses of channels 1 (0.6 μm), 2 (0.9 μm), 3 (3.7 μm), and of the Normalized Difference Vegetation Index (NDVI) combination of channels 1 and 2. A fire consumed 23% of the park's 1300 km² surface in August 1992; based on a subsequent Landsat Thematic Mapper image, three sub-areas that burnt were chosen for a detailed AVHRR comparative analysis with five sub-areas that did not burn. From the 344 images recorded on different days only 26 were effectively useful. Channel 1 showed little difference for burnt and unburnt vegetation. Channel 2 and NDVI displayed strong evidence of the fire for up to 13 months, while in channel 3 this period was less than 8 months. However, channel 3 and NDVI presented the strongest evidence of the fire occurrence on a short-term basis. The results support the use of AVHRR products based on channels 2 and 3 to monitor and evaluate the extent of vegetation burn and regrowth in savannas, important information for tropical vegetation.

1. Introduction

Savannas in Brazil, also known as *cerrados*, occupy about 1.8 M km², covering 20% of the country. They are usually found under a seasonal tropical climate (Nimer and Brandão 1989), with small average monthly temperature variations along the year. Rain distribution, however, is highly variable with two distinct seasons: a rainy one between November and March, and a dry one from May to September during the cooler winter period.

In the last few decades the *cerrados* underwent fast and uncontrolled occupation, mainly for agriculture and pasture expansion. Estimates for 1985 indicated that only 7% of its area was preserved, with 63% still covered by natural vegetation, though subject to different degrees of human interference (Dias 1990). More recently, Mantovani and Pereira (1998) used 164 Landsat Thematic Mapper (TM) images from 1985–1993 in a preliminary study and visually classified 30% of the *cerrados* as undisturbed. From another point of view, in a thorough study of Landsat images since 1973, França and Setzer (1997, 1999) showed that the Emas National Park, known as the least altered Brazilian *cerrado* reserve, burns almost completely once every 3 years as a result of anthropogenic fires.

Before human occupation Brazilian savannas survived in a fire-prone environment (Coutinho 1990), and lightning was the natural source of ignition. Their vegetation is therefore adapted to, and also dependent on, occasional fire. Coutinho (1990) stressed the role of fire in the nutrient cycle of the cerrados, which brings quick release of minerals by the above-ground phytomass and increases the amount of nutrients available for plants with superficial roots. Fire frequency also helps to shape the physiognomy and cerrado density, causing a more open savanna when more frequent. Many of the cerrado plants actually require fire to bud and blossom and without it their phenological cycle fails. Fire is also related to the shedding, spread and sprouting of seeds for various cerrado species.

The regular rise of fire in the cerrados is a common practice among peasants, farmers and cattle ranchers to open new areas, prevent natural vegetation regrowth, combat insects and weeds, to renew pastures, etc. The fire season usually starts in May and peaks by late August and early September after weeks or months of drought, with relative air moisture as low as 20%, and when dry phytomass and leaf shedding are at their maximum. Hundreds of thousands of fires of anthropogenic origin have been detected each year in the central Brazilian cerrados but their number is greatly reduced with the rains that are occasional in September and become regular in October (Climanálise 1992–98). It must be stressed that the frequency of man-originated fires of intentional, accidental or criminal motivation, in areas that are protected or not, is far greater than fires due to natural causes, and therefore rapidly transforms the original savanna environment.

The use of Advanced Very High Resolution Radiometer (AVHRR) data to estimate burnt areas started with the pioneering works of Malingreau *et al.* (1985) and Matson and Holben (1987); the subject has been thoroughly reviewed by Pereira *et al.* (1997) and a significant field validation effort in Africa using the Along Track Scanning Radiometer (ATSR) onboard the European ERS satellites was recently presented by Eva and Lambin (1998). The current stand is that AVHRR multi-temporal image analysis and AVHRR middle and near-infrared channels provide the most useful information to estimate burnt areas. These estimates reflect international scientific needs (UNEP/WMO 1995) requiring regular world-coverage products (Malingreau and Dwyer 1996).

This work examines the use of temporal sequences of AVHRR images to identify and monitor changes caused by fire to a typical Brazilian savanna vegetation in relation to neighbouring control areas not hit by fire. Additionally, a comparison of the burnt area estimates made with AVHRR and TM was made for the test site. The results of this simple approach should help the design of future operational products to monitor vegetation and land-use changes caused by fires based on AVHRR and forthcoming orbital sensors.

2. The Emas National Park

The Emas Park is located in a savanna, or cerrado, morphoclimatic environment in the central Brazilian plateau (Ab'Saber 1971) between 17° 49' and 18° 28' S and 52° 39' and 52° 10' W in the south-west of Goiás state. The elevation of its 1320 km² varies from 650 to 900 m. Prevailing vegetation types are 'campos limpos' (open grasslands) and 'campos sujos' (grasslands with intermediate and sparse shrubs); gully forests, swampy grass fields and eutrophic seasonal tropical forests are occasionally found. Figure 1 shows the park's location and a more detailed description of its vegetation and characteristics is found in França (1994) and França and Setzer (1997,

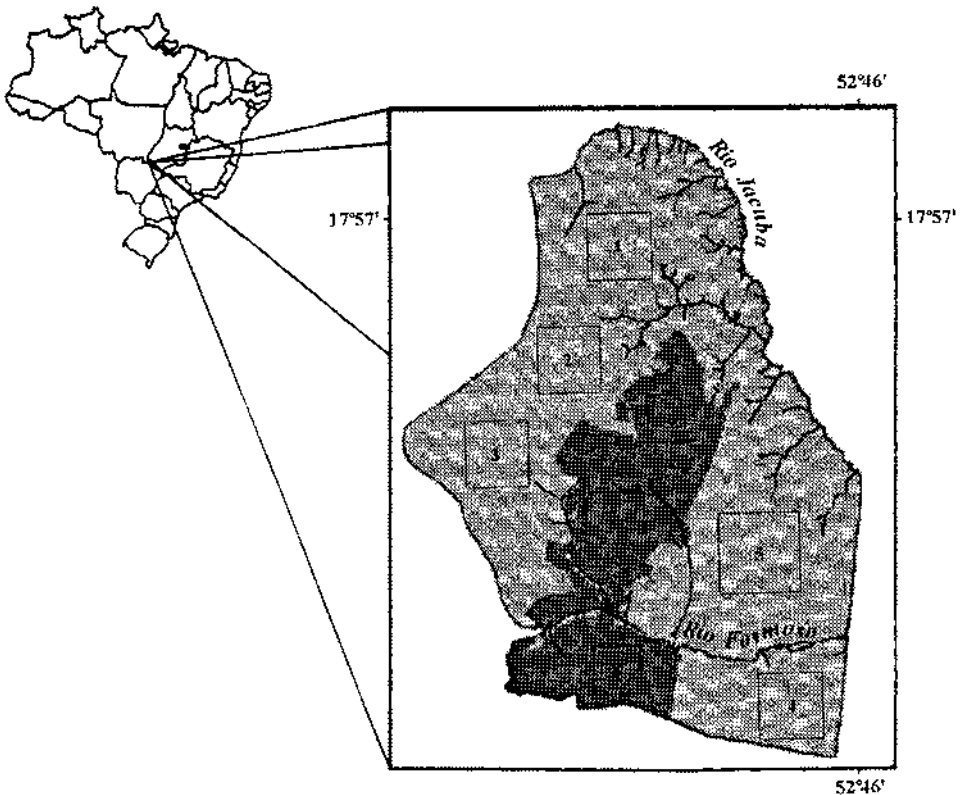


Figure 1. Location of the Emas National Park in central Brazil and of the eight sample areas used in the study.

1998). According to IBAMA (1989) Emas is the most important area preserved in the cerrados because of its large size and undisturbed environment, despite major fires that overrun the whole park every 3 years and small fires that affect it every year (França and Setzer 1997, 1999).

The park was established in 1961, and the large fires of 1966, 1975, 1978, 1985, 1988, 1991 and 1994 covered between 70 and 100% of its area. The fires in the beginning of August 1992 burnt 23% of the park, and the most recent fire, on August 1994, covered about 95% of the park (França and Setzer 1997, 1999). Figure 2 shows campos limpos, depicting a site hit by fire 1 year (figure 2(a)) and 2 years (figure 2(b)) after the fire of August 1992; prior to 1992 both sites burnt on September 1991.

3. Methodology

Eight sample areas in the park (see figure 1) were studied in a temporal sequence of AVHRR afternoon images from the NOAA-11 satellite, from 1 June 1992 until 8 October 1993; three of them, nos 6, 7 and 8, were in the section of the park that burnt on August 1992. The data for the other five areas used as control sites are the same as published in França and Setzer (1998). The analysis of the AVHRR images was based on the information in channels 1 (0.58–0.68 μm), 2 (0.72–1.1 μm) and 3 (3.55–3.93 μm). Integration of the AVHRR images with the sample areas contours

*(a)**(b)*

Figure 2. View of vegetation regrowth in the Park's study area (a) 1 year and (b) 2 years after the August 1992 fire.

was done using a Geographical Information System (GIS); the park limits and the sample areas were digitized from IBGE (1977, 1978) charts.

3.1. Sample areas

The vegetation in three Emas sample areas that burnt in the 1992 fire contained mainly campos limpos and campos sujos; this was concluded from the analysis of a Landsat TM image from 25 August 1992 (line/base 224/73 B+) at a scale of 1:100 000 using channels 3 ($0.6 \mu\text{m}$), 4 ($0.8 \mu\text{m}$) and 5 ($1.65 \mu\text{m}$) in a red–green–blue colour composite photographic enlargement supplied by the Brazilian Space Institute (INPE). Additionally, a field trip to the park on September 1993 corroborated the image interpretation and the fire occurrence. The five control areas not disturbed by the fire and their data are described in more detail in França and Setzer (1998).

3.2. Selection and treatment of the AVHRR NOAA-11 images

As described by França and Setzer (1998), 344 AVHRR images of the NOAA-11 afternoon overpasses were recorded by INPE at full 1.1 km resolution during the total period of 548 days studied. Only 26 images remained for the analysis after screening the Emas park region in each of these images for significant cloud cover, border distortion caused by large AVHRR scanning angles, and noisy signals. Using the GIS the sample areas defined in the Landsat TM scene shown in figure 1 were located in the images; their size ranged from 20 to 30 AVHRR pixels. Each sample area in the 26 images was further examined in detail in channel 2 and eliminated from the analysis when contamination caused by small cloud cover or shadow was detected.

The average value of the Digital Numbers (DNs) in the three channels was calculated for the sample areas identified as nos 6, 7 and 8. The average DNs were converted to radiance using the linear equations given by Kidwell (1993). The radiances were next compensated for the solar elevation angle (channels 1 and 2) and for the distance between the Earth and the Sun (channels 1, 2 and 3) at the time of the image acquisition. The compensated radiances were then converted back to DNs using the equations used by Kidwell (1993), and the Normalized Difference Vegetation Index (NDVI) was obtained from the resulting data for channels 1 and 2 using the relation $(\text{channel } 2 - \text{channel } 1)/(\text{channel } 2 + \text{channel } 1)$. NDVIs obtained either from DNs or radiance are accepted (Kidwell 1990) and, in fact, the linear transformation that converts one into another causes a negligible difference for the range between 0 and 0.4 that comprises vegetation responses (Setzer and Barbosa 1998). The conversion to albedos was necessary to allow for the compensations made. The use of DNs rather than radiances to analyse the AVHRR response has been a choice of the authors, as in França and Setzer (1998).

4. Results and discussion

Table 1 presents the average values for the three AVHRR channels and NDVI combination of channels 1 and 2 calculated for the eight sample areas in all 26 images studied. Images were scarcer in the rainy season because of prevailing cloud cover. In the graphs presented in figures 3–6, sample areas nos 1–5 and 6–8 were averaged to produce only two curves: one for the areas not affected by fire and another one for the areas that burnt. As described in França and Setzer (1998), significant changes in the signals of channels 1 and 2 in individual images resulted from variations in the AVHRR off-nadir scanning angle. These effects, caused solely

Table 1. AVHRR pixel data summary (channels 1, 2, 3 and NDVI) for three burnt areas and for five reference unburnt areas in the Emas National Park.

Year	Image	Day	Ave. 1–5	A6	A7	A8	Ave. 6–8	
Channel 1 1992	E1	152	29.5	—	—	—	—	
	E2	153	26.7	26.1	26.2	32.0	28.1	
	E3	159	35.7	35.2	35.1	37.5	35.9	
	E4	167	37.2	—	38.0	—	38.0	
	E5	186	28.8	—	—	—	—	
	E6	200	41.3	42.7	41.8	40.5	41.7	
	E7	201	35.0	35.1	35.1	35.1	35.1	
	E8	205	39.6	39.6	39.6	41.3	40.2	
	E9	211	29.5	29.5	29.5	29.6	29.5	
	E10	251	32.8	32.9	32.0	33.1	32.6	
	1993	E11	252	29.4	31.9	30.1	28.6	30.2
		E12	117	28.4	27.7	27.5	—	27.6
		E13	174	30.3	30.2	30.2	30.2	30.2
		E14	175	30.8	30.2	30.0	—	30.1
		E15	176	32.4	31.6	31.4	36.4	33.1
		E16	177	37.0	37.1	37.1	37.1	37.1
		E17	183	30.7	28.8	28.2	31.0	29.3
		E18	185	34.8	34.6	34.6	34.6	34.6
		E18	191	31.0	30.8	31.0	31.0	31.0
		E20	192	31.3	31.5	31.5	31.5	31.5
		E21	198	38.3	38.0	38.0	38.0	38.0
		E22	201	32.2	31.8	31.8	32.3	32.0
		E23	216	31.1	31.1	30.4	31.5	31.0
		E24	218	37.7	36.8	37.1	37.1	37.0
		E25	280	24.4	24.3	24.3	25.2	24.6
		E26	281	26.8	25.6	25.0	26.8	25.8
Channel 2 1992	E1	152	48.7	—	—	—	—	
	E2	153	47.3	48.7	49.5	47.6	48.6	
	E3	159	59.1	59.5	59.1	53.5	57.4	
	E4	167	59.5	—	60.3	—	60.3	
	E5	186	44.6	—	—	—	—	
	E6	200	56.9	57.8	57.4	50.9	55.4	
	E7	201	48.2	49.5	49.3	44.8	47.9	
	E8	205	50.7	51.4	51.8	47.2	50.1	
	E9	211	42.1	42.5	42.5	39.3	41.4	
	E10	251	42.5	43.1	43.6	40.2	42.3	
	1993	E11	252	40.5	36.2	34.7	33.5	34.8
		E12	117	46.8	49.8	48.4	—	49.1
		E13	174	46.2	49.0	46.6	50.2	48.6
		E14	175	41.8	44.5	44.4	—	44.4
		E15	176	45.3	48.9	48.8	54.3	50.7
		E16	177	53.0	57.4	58.0	58.8	58.1
		E17	183	42.0	44.8	44.6	46.9	45.4
		E18	185	49.4	53.1	53.6	55.4	54.1
		E18	191	41.5	43.6	41.9	46.1	43.8
		E20	192	42.7	46.4	45.7	46.5	46.2
		E21	198	49.5	52.0	53.2	54.1	53.1
		E22	201	44.7	48.9	49.2	50.1	49.4
		E23	216	40.2	42.8	42.7	44.9	43.5
		E24	218	47.6	51.0	50.9	52.5	51.5
		E25	280	35.9	38.4	38.9	40.7	39.4
		E26	281	44.4	46.3	46.6	49.2	47.4

Table 1. (Continued).

Year	Image	Day	Ave. 1–5	A6	A7	A8	Ave. 6–8
Channel 3 1992	E1	152	139.3	—	—	—	—
	E2	153	135.4	136.6	136.6	126.5	133.2
	E3	159	134.9	135.4	137.7	129.0	134.1
	E4	167	140.0	—	142.1	—	142.1
	E5	186	122.7	—	—	—	—
	E6	200	136.1	136.6	137.5	133.1	135.7
	E7	201	124.4	125.9	125.1	123.3	124.7
	E8	205	129.9	130.3	130.6	127.7	129.6
	E9	211	107.6	107.6	107.9	108.0	107.8
	E10	251	107.1	59.7	59.5	58.2	59.1
1993	E11	252	98.1	47.0	45.8	42.5	45.1
	E12	117	139.4	139.4	138.2	—	138.8
	E13	174	144.8	144.6	144.6	144.9	144.7
	E14	175	143.0	144.5	144.3	—	144.4
	E15	176	138.3	139.7	139.5	135.6	138.3
	E16	177	135.6	137.9	137.1	137.6	137.5
	E17	183	136.1	138.2	136.8	135.7	136.9
	E18	185	127.1	128.8	128.4	129.1	128.8
	E18	191	134.8	134.7	133.5	134.4	134.2
	E20	192	133.4	134.8	134.0	135.2	134.6
	E21	198	138.2	139.2	138.5	137.4	138.3
	E22	201	127.0	128.2	126.4	127.1	127.2
	E23	216	119.0	119.2	118.8	118.0	118.7
	E24	218	113.9	115.0	113.5	113.5	114.0
	E25	280	124.8	128.2	128.6	127.3	128.0
	E26	281	111.6	115.2	116.2	115.4	115.6
NDVI 1992	E1	152	0.25	—	—	—	—
	E2	153	0.28	0.30	0.31	0.20	0.27
	E3	159	0.25	0.26	0.25	0.18	0.23
	E4	167	0.23	—	0.23	—	0.23
	E5	186	0.21	—	—	—	—
	E6	200	0.16	0.15	0.16	0.11	0.14
	E7	201	0.16	0.17	0.17	0.12	0.15
	E8	205	0.12	0.13	0.13	0.07	0.11
	E9	211	0.18	0.18	0.18	0.14	0.17
	E10	251	0.13	0.14	0.15	0.10	0.13
1993	E11	252	0.16	0.06	0.07	0.08	0.07
	E12	117	0.24	0.29	0.27	—	0.28
	E13	174	0.21	0.24	0.21	0.25	0.23
	E14	175	0.15	0.19	0.19	—	0.19
	E15	176	0.17	0.22	0.22	0.20	0.21
	E16	177	0.18	0.21	0.22	0.23	0.22
	E17	183	0.16	0.22	0.23	0.20	0.22
	E18	185	0.17	0.21	0.22	0.23	0.22
	E18	191	0.15	0.17	0.15	0.19	0.17
	E20	192	0.15	0.19	0.18	0.19	0.19
	E21	198	0.13	0.16	0.17	0.18	0.17
	E22	201	0.16	0.21	0.21	0.22	0.21
	E23	216	0.13	0.16	0.17	0.18	0.17
	E24	218	0.12	0.16	0.16	0.17	0.16
	E25	280	0.19	0.22	0.23	0.23	0.23
	E26	281	0.25	0.29	0.30	0.30	0.30

by the viewing sensor–target–sun geometry, were not compensated, and their role was assumed to be the same in all the sample areas of a single image. These figures also have straight lines connecting the signal values obtained in the individual images; in reality, if the missing temporal data could also be included the lines would not be straight.

4.1. Channel 1

As seen in figure 3 and table 1, only minor differences are apparent between the signals of the burnt and unburnt sample areas in channel 1 ($0.58\text{--}0.68\ \mu\text{m}$) of the AVHRR images E10 and E11 already include the effect of the large fire of August 1992, and for about 1 month the DN_s (or radiances) in the burnt areas were slightly higher than in the unburned control areas, indicating that the removal of the leaves with consequent larger exposure of soil tends to increase the light reflection and the sensor signal. Conversely, image E12 at the end of the rainy season in 1993 shows slightly smaller DN_s for the areas burnt in the previous year; this possibly results from the stronger absorption of light by green vegetation that replaced the dry and brighter leaves. Figures 2(a) and 2(b) depict such conditions in the field, where the latter, obtained 1 year after the fire, shows darker and less reflective grass.

4.2. Channel 2

The signal of channel 2 ($0.72\text{--}1.1\ \mu\text{m}$) of the AVHRR presented a much wider temporal variation than that in channel 1, as shown in figure 4 and table 1. Image E11, acquired after the fire and with the Emas Park close to nadir, showed lower DN_s (or radiances) for the burnt areas, when no healthy vegetation existed to reflect near-infrared radiation. It is important to note that after image E11, following the recovery of the burnt vegetation, until the end of the period studied, the burnt areas

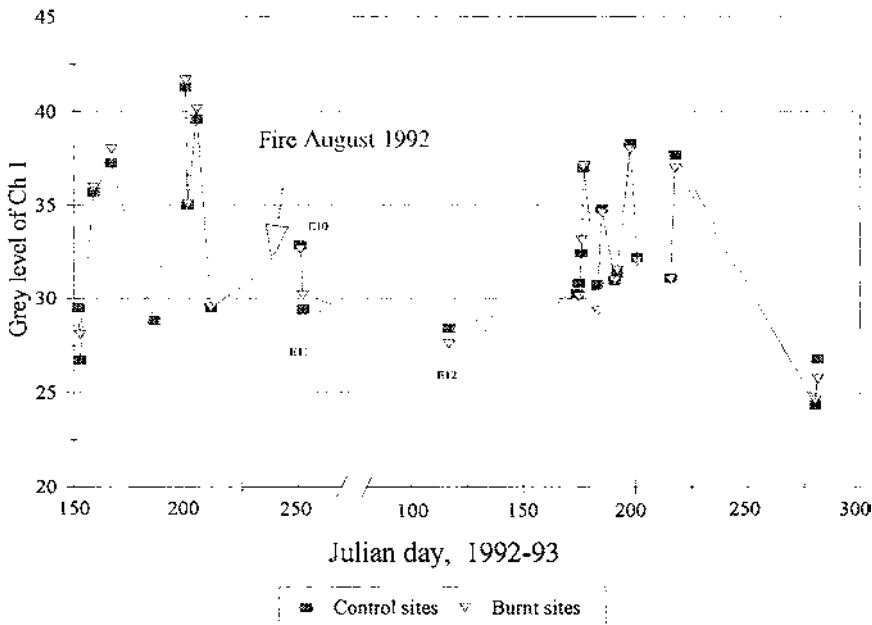


Figure 3. Comparison of the AVHRR channel 1 ($0.6\ \mu\text{m}$) temporal response for the burnt and unburnt sample areas in the Emas National Park.

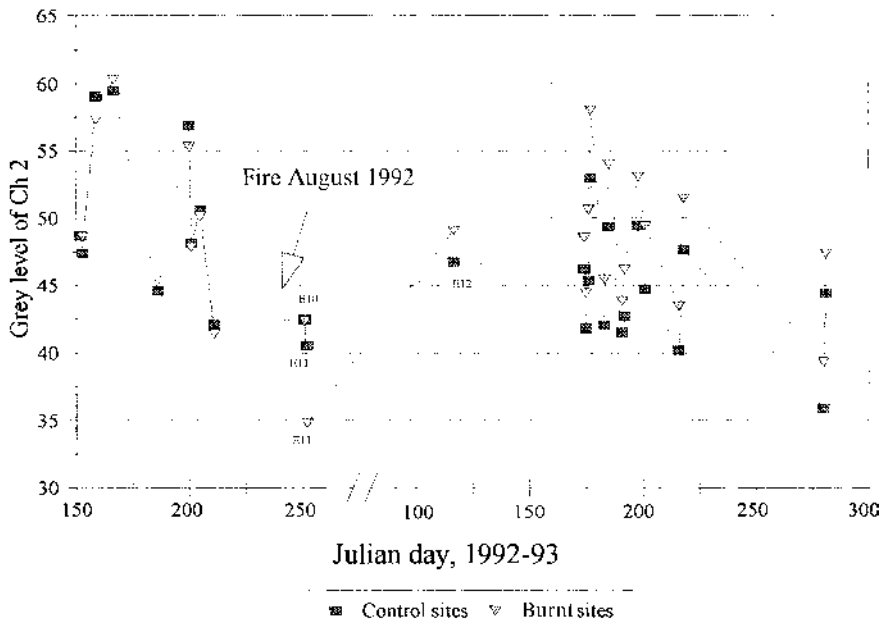


Figure 4. Comparison of the AVHRR channel 2 ($0.9\ \mu\text{m}$) temporal response for the burnt and unburnt sample areas in the Emas National Park.

showed a stronger signal in channel 2 compared to the unburnt control sites. As seen in figure 2(b) for the unburned vegetation, this resulted mainly from the near-infrared light absorption by the older vegetation, and also from the reduction in the amount of exposed soils.

Image E11 was acquired just 1 day after E10, and both refer to the post-burn period in the park. As seen in figure 5, although the burnt and unburned areas display basically the same channel 2 sensor signal value in E10, a significant difference exists in E11. A similar condition is also found for these same areas in channel 1 (see figure 4). Such day-to-day variations in the AVHRR sensor signals result from changes in the sensor viewing geometry and the Sun's position in relation to the target, and also from the target spectral characteristics. Rahman (1996), in his modelling work, and França and Setzer (1998), using actual AVHRR data, have stressed the presence of these signal variations but, in general, analyses of AVHRR channels 1 and 2 images in the literature still neglect the necessary care or corrections needed.

4.3. Channel 3

Compared to the other two channels, channel 3 ($3.55\text{--}3.93\ \mu\text{m}$) presented the wider signal variation in time for both burnt and unburned areas (see figure 5 and table 1). On image E9, before the fire, the average DN for the sample was 115.3; 1 month after the fire, on image E11, it still was 48.8 for the burnt areas, or about 58% less. Also, the visual identification and mapping of the burnt areas was best done using channel 3. This is interpreted as resulting from the increase in both the soil temperature and reflectance caused by the removal of the vegetation since channel 3 is sensitive to emitted and reflected radiation (Kaufman and Remer 1994,

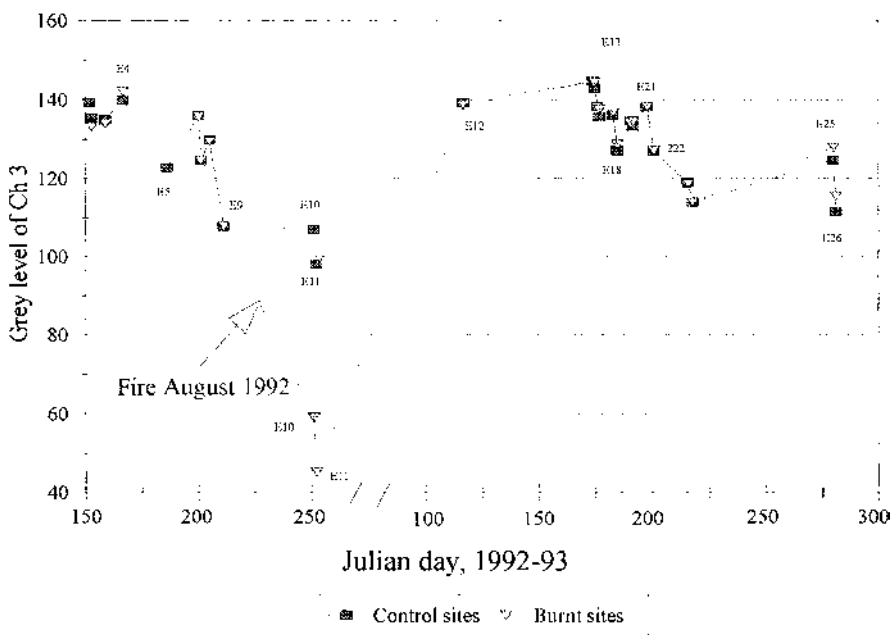


Figure 5. Comparison of the AVHRR channel 3 ($3.7\ \mu\text{m}$) temporal response for the burnt and unburnt sample areas in the Emas National Park.

Setzer and Verstraate 1994). This combined signal presents great potential in vegetation studies but for unknown reasons is seldom used. Reduced DNs in this channel, as a result of the inverted scale provided by the sensor, indicate increased temperatures (Kidwell 1993). After day 117 of 1993 (231 days after the fire), when the soil was again mostly covered by vegetation (figure 2(a)), no differences in signal were noticeable between the burnt and unburned areas (see figure 5).

4.4. NDVI

The temporal sequence of the AVHRR-derived NDVI, also showed very clearly the effect of the fire in the sample areas nos 6–8 (see figure 6 and table 1). Comparing the data of image E9 before the fire with those of image E11 after the fire, the NDVI dropped by 59% with the burning of the vegetation. However, on image E12 from day 117, by the end of the rainy season of 1993, the NDVI values were higher for the burnt areas. As expected, this indicates a stronger growth of the photosynthetically active vegetation in the burnt areas. In other words, NDVI will show low values for fire scars until a first rain occurs, when the sprouting vegetation will significantly increase its values; nevertheless, even after such rains, the NDVI curves for burnt and non-burnt sites will show for a long period a marked difference that is not found in the individual signal of channels 1 and 3.

Kasischke and French (1995) and Martin and Chuvieco (1994) have used AVHRR NDVI temporal data to map the extent of burnt areas in boreal and Mediterranean regions, respectively. Their approach involved comparison of early and late season images for a single year, and the area estimates were dependent on the classification thresholds used. In general, their NDVI burn patterns were similar to those of our work, but a longer and more numerous sequence of images such as the one we

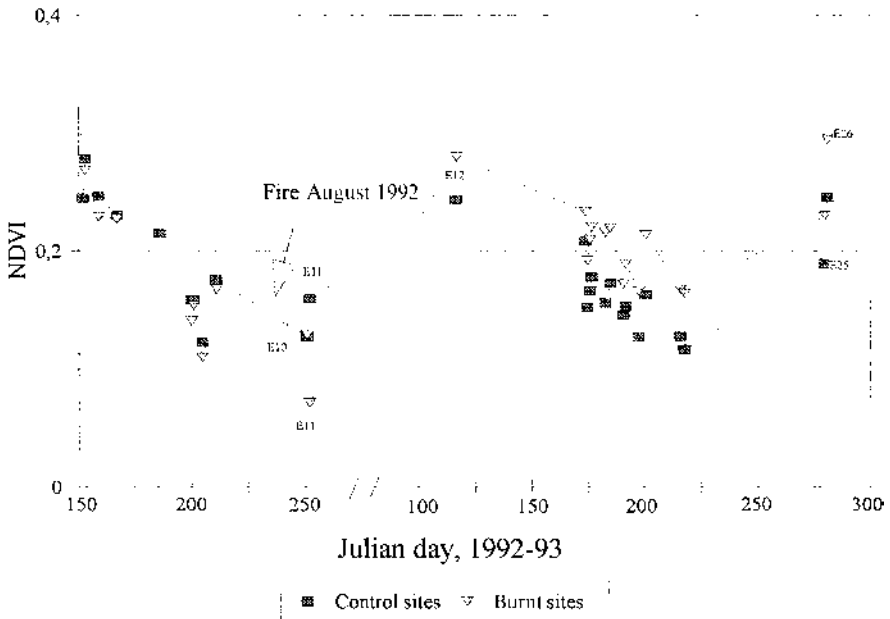


Figure 6. Comparison of the AVHRR NDVI temporal response for the burnt and unburnt sample areas in the Emas National Park.

present provides a more detailed insight of the temporal changes of the vegetation and imaging conditions regarding a fire event.

4.5. Evaluation of the burnt area

An evaluation of the extent of the area burnt in the Emas Park was made using channel 3 data, where the contrast with the unburnt vegetation was the strongest. The image used was E11, acquired 27 days after the fire, in which pixels with DN's between 52 and 90 (in an 8-bit 256 level scale) corresponded to the fire scar signature. The area obtained was 253 km², in comparison to the value of 300 km² measured through the photo-interpretation of the TM image from 25 August 1992 (França and Setzer 1997, 1999, Hlavka *et al.* 1996); thus, AVHRR in this case, with its nadir resolution of 1.1 km, underestimated the fire scar by 15.7% in relation to the 30 m TM high resolution image.

5. Conclusions

A major gap in studies of savannas is the lack of information about the extent of areas burnt. This work showed for a savanna test area in Brazil that 1.1 km resolution daily AVHRR images can be used to detect large fire scars and to monitor the ensuing vegetation recovery. Although the period studied had 548 days, only 26 useful images for the area of interest had clear skies or adequate scanning angles; such practical limitations tend to be neglected by most users of satellite data, but fortunately do not prevent studying the effects of fire. For instance, changes caused by fires could be identified in channel 2 and NDVI images up to 13 months after the fires; channel 3 data, which proved to be the best at detecting the scars, will outperform other channels even 1 month after the fire has occurred.

The results presented strengthen the possibility of developing must-needed operational products to monitor the extent and effects of fire in savannas. Historic databases of fire use for a few decades could be produced and coupled to fire products expected to be generated by forthcoming sensors like MODIS.

Acknowledgements

The authors acknowledge the partial support received through grants FAPESP 93/1737-1 and CNPq No. 300.557/97-3.

References

- AB'SABER, A. N., 1971, A organização natural das paisagens inter e subtropicais brasileiras. In *Simpósio sobre o cerrado*, 3., edited by M. G. Ferri (São Paulo: E. Blücher/Edusp), pp. 1–14 (in Portuguese).
- CAETANO, M., MERTES, L., CADETE, L., and PEREIRA, J., 1996, Assessment of AVHRR data for characterizing burned areas and post-fire vegetation recovery. *EARSeL Advances in Remote Sensing*, **4**, 124–134.
- CLIMANÁLISE, 1992–98, Climanálise Weather Report. CPTEC/INPE, C. Paulista.
- COUTINHO, L. M., 1990, Fire in the ecology of the Brazilian cerrado. In *Fire in the Tropical Biota*, Ecological Studies, 84, edited by J. G. Goldammer (New York: Springer-Verlag), pp. 82–105.
- DIAS, B. F. S., 1990, A conservação da natureza. In *Cerrado: caracterização, ocupação e perspectivas*, edited by M. N. Pirt (Brasília: UnB), pp. 583–640 (in Portuguese).
- EVA, H., and LAMBIN, E. F., 1998, Burnt area mapping in central Africa using ATSR data. *International Journal of Remote Sensing*, **19**, 3473–3497.
- FRANÇA, H., and SETZER, A. W., 1997, Regime de queimadas no Parque Nacional das Emas: 1793–95. Report to FAPESP-grant 95/2674-9 (in Portuguese), 86 pp.
- FRANÇA, H., and SETZER, A. W., 1998, AVHRR temporal analysis of a savanna site in Brazil. *International Journal of Remote Sensing*, **19**, 3127–3140.
- FRANÇA, H., and SETZER, A. W., 1999, As queimadas no Parque Nacional das Emas. *Ciência Hoje*, **26**, 69–73 (in Portuguese).
- HLAVKA, C. A., AMBROSIA, V. G., BRASS, J. A., REZENDEZ, A. R., and GUILD, L. S., 1996, Mapping fire scars in the Brazilian cerrado using AVHRR imagery. In *Biomass Burning and Global Change*, edited by J. S. Levine (London: MIT Press), pp. 555–560.
- IBAMA, 1989, Instituto Brasileiro de Meio Ambiente e dos Recursos Naturais Renováveis. *Unidades de conservação do Brasil* (Brasília: IBAMA) (in Portuguese).
- IBGE, 1977, Instituto Brasileiro de Geografia e Estatística. Charts SE-22-V-C-VI.
- IBGE, 1978, Instituto Brasileiro de Geografia e Estatística. Charts SE-22-Y-A-III, SE-22-Y-A-II.
- KAUFMAN, Y. J., and REMER, L. A., 1994, Detection of forests using mid-IR reflectance: an application for aerosol studies. *IEEE Transactions on Geoscience and Remote Sensing*, **32**, 672–683.
- KASISCHKE, E. S., and FRENCH, N. H., 1995, Locating and estimating the areal extent of wildfires in Alaskan boreal forests using multiple-season AVHRR NDVI composite data. *Remote Sensing of Environment*, **51**, 263–275.
- KIDWELL, K. B., 1990, *Global Vegetation Index: User's Guide* (NOAA: Washington, DC).
- KIDWELL, K. B., 1993, *NOAA Polar Orbiter Data: User Guide (Tiros-N, NOAA-6 through NOAA-12)* (NOAA: Washington, DC).
- MALINGREAU, J. P., STEVENS, G., and FELLOWS, L., 1985, The 1982–83 forest fires of Kalimantan and North Borneo: satellite observations for detection and monitoring. *Ambio*, **14**, 314–321.
- MALINGREAU, J. P., and DWYER, E., 1996, A framework for the presentation and analysis of the Global Fire Product. In *The IGBP-DIS fire algorithm workshop, II*, edited by C. O. Justice and J. P. Malingreau (France: Toulouse).
- MARTIN, M. P., and CHUVIECO, E., 1994, Mapping and evaluation of burned land from multitemporal analysis of AVHRR NDVI images. *Proceedings of the International Workshop on Satellite Technology and GIS for Mediterranean Forest Mapping and Fire*

- Management, Thessaloniki, Greece, November 1993, JRC/AUTH/EARSeL, edited by P. J. Kennedy and M. Kartesis (Luxembourg European Commission-DG-3), pp. 71–83.*
- MATSON, M., and HOLBEN, B., 1987, Satellite detection of tropical burning in Brazil. *International Journal of Remote Sensing*, **8**, 509–516.
- MATOVANI, J. E., and PEREIRA, A. C., 1998, Estimativa da integridade da cobertura vegetal de cerrado através de dados TM/Landsat. *Anais do IX Simpósio Brasileiro de Sensoriamento Remoto*, Santos, 11–18 September 1998, 12 pp. CD-ROM INPE e SELPER, São José dos Campos (in Portuguese).
- NIMER, E., and BRANDÃO, A. M. P. M., 1989, *Balanço hídrico e clima da região dos cerrados* (IBGE: Rio de Janeiro) (in Portuguese).
- PEREIRA, J. M. C., CHUVIECO, E., BEAUDOIN, A., and DESBOIS, N., 1997, Remote sensing of burned areas: a review. In *A Review of Remote Sensing Methods for the Study of Large Wildland Fires*, edited by Emilio Chuvieco (Spain: Alcalá de Henares), pp. 127–183.
- RAHMAN, H., 1996, Atmospheric optical depth and water vapour effects on the angular characteristics of surface reflectance in NOAA AVHRR. *International Journal of Remote Sensing*, **17**, 2981–2999.
- SETZER, A., and BARBOSA, H. A., 1998, Índice de vegetação AVHRR: melhor simplificar seu cálculo! *X Congresso Brasileiro de Meteorologia, Brasília*. Anais, CD-ROM, 5 pp.
- SETZER, A. W., and VERSTRATE, M. M., 1994, Fire and glint in AVHRR's channel 3: a possible reason for the non-saturation mystery. *International Journal of Remote Sensing*, **15**, 711–718.
- UNEP/WMO, 1995, The United Nations Framework Convention on Climate Change. Chatelaine, Switzerland, IUCC, United Nations Environmental Program.